





## Future climate change will increase risk to mangrove health in Northern Australia

Christine T. Y. Chung <sup>1</sup>✉, Pandora Hope<sup>1</sup>, Lindsay B. Hutley <sup>2</sup>, Josephine Brown <sup>3</sup> & Norman C. Duke <sup>4</sup>

Mangroves of the wet-dry tropical Gulf of Carpentaria, Australia, survive in a harsh environment. One of the worst recorded mangrove dieback events occurred during the El Niño of 2015 following an extreme, two-year sea level drop, illustrating that enhanced climate variability can exacerbate major stressors for these ecosystems. As well as sea level variability, maximum daily temperatures in the Gulf of Carpentaria are also linked to climate variability and change, and may play an important role in overall mangrove health. Here we address how these two factors: sea level variability and maximum daily temperatures, are projected to change under several future emissions scenarios. Climate projections from the sixth generation of Coupled Model Intercomparison Project indicate an increased occurrence of anomalously low and high sea level events in the coming century. This, alongside enhanced temperature stress, is likely to significantly increase risk to mangrove health in this region. The rate of increase of low and high sea level events, and high temperature events, is scenario-dependent, and is largest for a high-emissions scenario.

<sup>1</sup>Bureau of Meteorology, Melbourne, Australia. <sup>2</sup>Research Institute for the Environment and Livelihoods, Charles Darwin University, Darwin, Australia.

<sup>3</sup>School of Geography, Earth and Atmospheric Sciences, University of Melbourne, Melbourne, Australia. <sup>4</sup>Centre for Tropical Water and Aquatic Ecosystem Research, James Cook University, Townsville, Australia. ✉email: [christine.chung@bom.gov.au](mailto:christine.chung@bom.gov.au)

Globally, mangroves are an important coastal ecosystem, supporting critical biodiverse habitats, storing carbon, stabilising coasts and protecting coastal communities<sup>1</sup>. Regionally, mangrove distribution, extent, composition and biomass are primarily influenced by temperature and rainfall<sup>2</sup>. In 2015, ~8000 ha of mangroves along the coasts of the wet-dry tropical Gulf of Carpentaria (GoC; Fig. 1a) in northern Australia were impacted by a mass dieback event, and millions of mangrove trees died<sup>2,3</sup> (Fig. 1b). Research shows the dieback was triggered by cumulative stress induced by a severe, 2-year anomalous drop in sea level and high evaporative stress associated with the ‘stalled’ El Niño of 2014/15 and the following strong El Niño of 2015/16<sup>3,4</sup>. The low mean sea level across the GoC persisted for ~6 months and greatly restricted tidal ingress, resulting in a lethal increase in sediment salinity<sup>3–5</sup>. The 18.6-year lunar cycle may have also exacerbated the sea-level drop<sup>6</sup>. El Niño events are associated with lower sea level in the GoC, while La Niña events are associated with higher sea level<sup>7</sup>. During the months at which ENSO peaks (December–February), maximum daily air temperature ( $T_{\max}$ ) in the GoC is also significantly correlated to El Niño Southern Oscillation (ENSO), with higher temperatures observed during El Niño years. Although  $T_{\max}$  is not considered to be a trigger for mangrove dieback, it plays a compounding role in overall mangrove health<sup>2,8</sup>. From mid-2015 till mid-2016, minimum sea level in the western GoC was 0.1–0.2 m lower than usual (Fig. 1c), with the southern GoC experiencing sea level anomalies of up to 0.4 m below climatological values<sup>2,4</sup>. During the wet seasons (January–April) of 2015 and 2016, precipitation

was also anomalously low, while  $T_{\max}$  was anomalously high (Fig. 1d), with daily  $T_{\max}$  exceeding 40 °C in nearby Centre Island (Supplementary Fig 1).

This study addresses how stressors, particularly extreme sea level variability and  $T_{\max}$ , are projected to change in future and whether increased variability in El Niño Southern Oscillation (ENSO) might contribute to further stress. While this study is motivated by the dieback event, the projected changes to sea level and  $T_{\max}$  impact mangrove health more generally. Using models from the sixth phase of the Coupled Model Intercomparison Project (CMIP6), we show that under mid-range and high emissions scenarios, both sea level variability and  $T_{\max}$  are projected to increase significantly. These increases are significantly larger under the high emissions scenario.

While severe stress for mangroves arises from multi-month extreme sea level anomalies<sup>9–11</sup>, long-term sea level rise also presents an ongoing threat. In the GoC there is a hypothesis that the mangroves have extended inland in response to rapidly rising sea levels over recent decades<sup>2,7,8,12</sup>. Regionally, this is the most rapid sea level rise since the late 1700s<sup>13</sup>. The three decades preceding the 2015 dieback event were also relatively wet. These higher moisture conditions may have left the mangroves particularly vulnerable to the sudden sea level drop in 2015<sup>14</sup>. In addition to the long-term sea level rise, there is also a risk of drowning dieback events which are linked to anomalously high sea level events<sup>3,15</sup> and/or extended hydroperiod<sup>16,17</sup>. In the GoC, the seasonal cycle induces large changes in sea level of up to 0.5 m, with the lowest sea levels occurring during May–October,

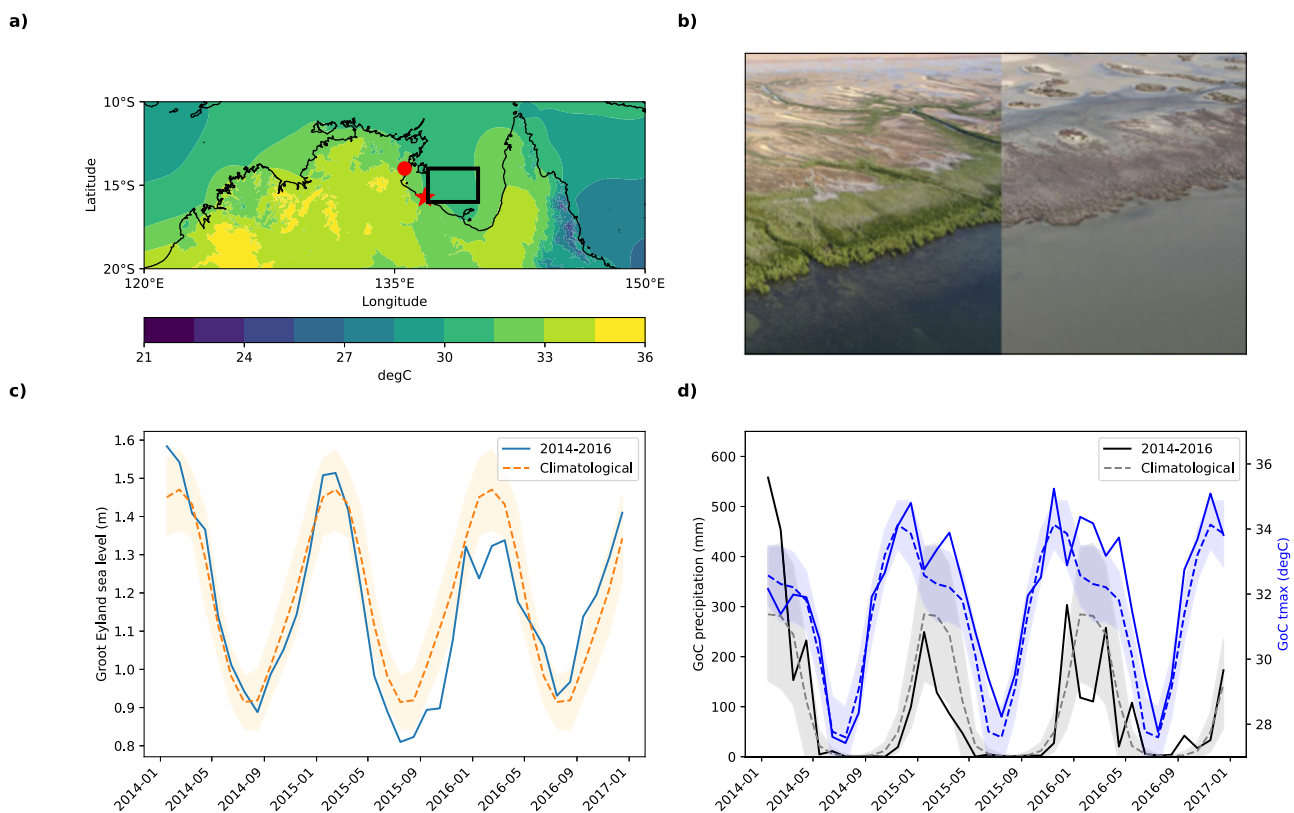


**Fig. 1** Rainfall and maximum temperatures during the 2015 dieback event relative to the climatology of the Gulf of Carpentaria. **a** Annual mean maximum daily temperatures averaged over 1950–2020. The Gulf of Carpentaria region used in this study is indicated by the black box. Red circle indicates the location of the Groote Eylandt station, and red star indicates the location of the Centre Island station. **b** Image comparing mangroves before and after the 2015 dieback event (image by Norman Duke) **c** Monthly mean sea level in the Groote Eylandt station in the western GoC from 2014–2016 (solid) as compared to the 1994–2019 climatological seasonal cycle (dashed). Shading indicates  $\pm 1$  standard deviation around the climatological values. **d** Monthly mean rainfall (black solid) and maximum daily temperature (blue solid) in the GoC region from 2014–2016 as compared to the 1950–2020 climatological seasonal cycle (dashed). Shading indicates  $\pm 1$  standard deviation around the climatological values.

and highest during November–April (Fig. 1c). We define stressful sea level conditions as unusually low sea levels during May–October, or unusually high during November–April or when either are present for extended periods of time (e.g. two years). We note that while tidal cycles play an important role<sup>6</sup>, global climate models do not typically simulate tides. Therefore in this study, we analyse monthly-mean sea level variability, which modulates the tidal cycle.

Mangroves in this region are likely to be growing near the climatological limit of their distributions, which is reflected in the relatively low diversity of these strands, with only three to four species commonly occurring<sup>3,8</sup>. In comparison, cooler and wetter regions in northern Australia such as Darwin Harbour are home to over 35 mangrove species<sup>18,19</sup>. Each year the mangroves of the GoC experience a strong seasonal decline in canopy cover<sup>4</sup> from September to December, a period of extremely low rainfall, high temperatures and seasonally low sea level<sup>1,2</sup> (Fig. 1c, d). The physiological limits of mangroves prevent them from effectively photosynthesizing when inland  $T_{\max}$  and sea-surface temperatures exceed a certain threshold, typically  $\sim 35^{\circ}\text{C}$  and  $32^{\circ}\text{C}$ , respectively<sup>8,20–24</sup>. Over the ocean in the GoC,  $T_{\max}$  peaks at  $\sim 34^{\circ}\text{C}$  climatologically (Fig. 1a, d). Additionally,  $T_{\max}$  at the nearby Centre Island weather station is often close to or above  $35^{\circ}\text{C}$  (Supplementary Fig 1a), suggesting that the mangrove communities in the GoC are able to withstand temperatures slightly higher than  $35^{\circ}\text{C}$ , but live in a highly stressful environment, particularly away from water courses. A recent study<sup>22</sup> found that most populations of *Avicennia marina*, the predominant species in the GoC, occur between  $T_{\max}$  of  $22\text{--}37^{\circ}\text{C}$ , and no instances of this species anywhere when  $T_{\max}$  exceeds  $37^{\circ}\text{C}$ . Throughout the dry May–September season, temperatures are usually cooler, with monthly averages of  $\sim 26^{\circ}\text{C}$  but the trees are more stressed from lower sea levels and low rainfall (Fig. 1d). Unusually high temperatures can compound that stress<sup>21</sup>, and any one month where  $T_{\max}$  exceeds these thresholds can contribute to reduced greenness<sup>4,22</sup>.

In this study, sea level variability and  $T_{\max}$  in the GoC are analysed from 15 models run under three standard CMIP6<sup>25</sup> scenarios: Historical (1900–2014), SSP245 (mid-range emissions future; 2015–2100), and SSP585 (high emissions future; 2015–2100) scenarios. For each scenario, CMIP6 models are run with a uniform set of time-varying greenhouse gas and aerosol inputs (see Methods for further details)<sup>26</sup>. This ensures that each model is responding to the same set of climate forcings, and that any variation in response is due to the models' internal variability and configuration.

## Results and discussion

To establish confidence in the models' future projections, an important first step is to evaluate the CMIP6 models' skill in simulating the observed seasonal cycle. As we examine only the risk arising from sea level variability around the mean rather than ongoing trends, we do not use the absolute sea level height from the CMIP6 models. Instead, we use the zos variable, which is the modelled dynamic sea level above geoid (see Methods for further details). This variable (zos) represents the variation from the global mean sea level at any given time, and is used as a proxy for sea level variability. The seas of the GoC are shallow and tend to vary together<sup>27,28</sup>, so an average over the region in Fig. 1a is representative of the whole basin's variability. To check the models' ability to simulate the seasonal cycle in the GoC, zos over the Historical period is compared to the observed sea level height from the Groot Eyland station (Fig. 2a). Although zos is not equal to absolute sea level height and should not be read as such, Fig. 2a shows that the models do accurately capture the seasonal cycle of

monthly mean sea level. One important feature to note about zos is that it does not reflect long-term sea level rise, as it is defined relative to the global mean at any given time.

For  $T_{\max}$ , the model output averaged over the GoC region is compared directly to observations of  $T_{\max}$  from the Australian Gridded Climatology Dataset (AGCD) averaged over the same region. Unlike zos, the modelled  $T_{\max}$  does reflect the long-term warming trend, as it is an absolute quantity. While the CMIP6 models accurately capture the seasonal cycle of  $T_{\max}$  (Fig. 2b), the modelled  $T_{\max}$  values GoC are around 2–3 degrees cooler than the observed AGCD climatology. This underestimation of the maximum temperature range is important as it indicates that an absolute threshold cannot be applied directly in the analysis of the CMIP6 models. In fact, none of the models exceed  $T_{\max}$  of  $35^{\circ}\text{C}$  in the historical or SSP245 scenarios, in any year. To account for this, two definitions of a high temperature year are applied—firstly using a  $T_{\max}$  threshold relative to each model's own climatology and standard deviation for each scenario, and secondly using an absolute  $T_{\max}$  threshold of  $32^{\circ}\text{C}$  (see Methods for details). The relative threshold accounts for any acclimatisation or species change that might occur as global temperatures warm in future as it only counts  $T_{\max}$  that exceed 1 standard deviation above climatological values for each future scenario. Note that the use of these thresholds in this study are to allow us to quantify the change in the frequencies of high  $T_{\max}$  events. They may not correspond exactly to the GoC species temperature thresholds, but provide a statistical means to quantify the increase in future stress events.

CMIP6 models also reproduce well the observed Historical relationship between ENSO and sea level in the GoC during December–February (DJF) when ENSO peaks (Fig. 2c), providing confidence in the models' assessment of how that relationship might change. ENSO variability is projected to increase under future scenarios<sup>29</sup>, as does zos (modelled dynamic sea level above geoid) variability, with a larger increase occurring under SSP585. In zos, a systematic shift towards more positive skewness in SSP585 compared to Historical indicates a tendency towards more moderate negative sea level anomalies and higher positive sea level anomalies. Both SSP245 and SSP585 Niño3.4 distributions indicate a tendency towards stronger El Niños and La Niñas. The relationship between zos and Niño3.4 also holds during the dry season (shown for August–October in Supplementary Fig 2a).

A clear shift to higher  $T_{\max}$  from Historical to SSP585 is projected, however models do not accurately capture the strong DJF correlation between  $T_{\max}$  and the Niño3.4 index (sea surface temperatures averaged across  $5^{\circ}\text{S}\text{--}5^{\circ}\text{N}$ ,  $170^{\circ}\text{W}\text{--}120^{\circ}\text{W}$ ; Fig. 2d). Thus, it is difficult to ascertain the projected influence of increased ENSO variability on  $T_{\max}$  variability. There is no significant correlation, observed or modelled, between  $T_{\max}$  and Niño3.4 in other seasons (March–November; see Supplementary Fig 2b for August–October).

To quantify future risk to mangrove health, occurrence rates of low and high sea level events and high  $T_{\max}$  events are calculated. Low and high sea level events are defined to be when zos are smaller or larger than one standard deviation of the monthly climatology (see Methods for further details). Again, this is not meant to be an exact threshold at which mangroves decline, but a statistical means to quantify the change in frequency of events. The relative threshold-based method (Fig. 3a) takes into account the increase in  $T_{\max}$  variability in future scenarios, thus yields fewer high  $T_{\max}$  years overall. Both future scenarios show statistically significant increases in high  $T_{\max}$  events, with SSP585 having more than double the instances of high relative  $T_{\max}$  than SSP245. Using the absolute threshold method (Fig. 3b), there is an even larger, significant increase in both future scenarios. Due

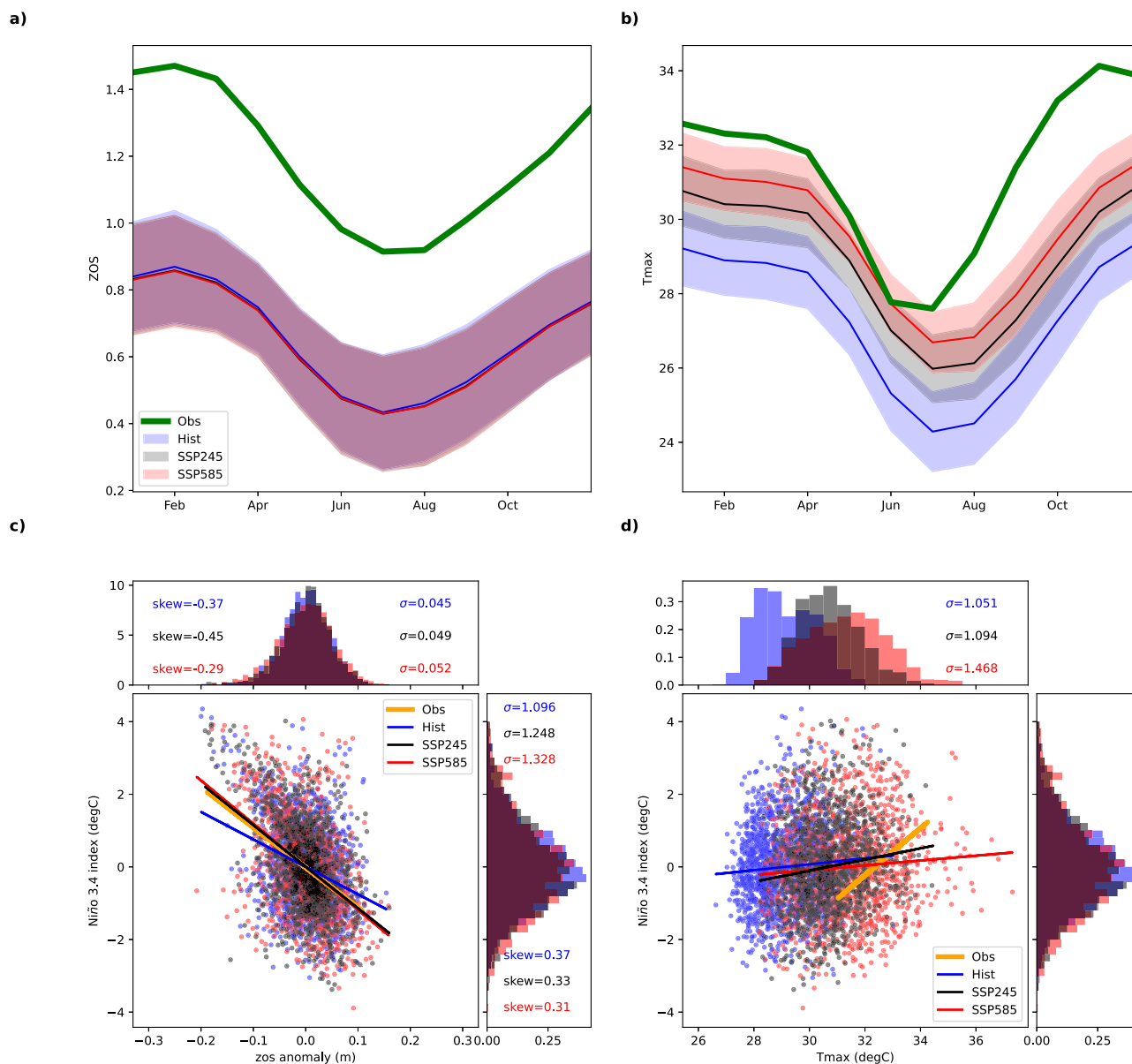


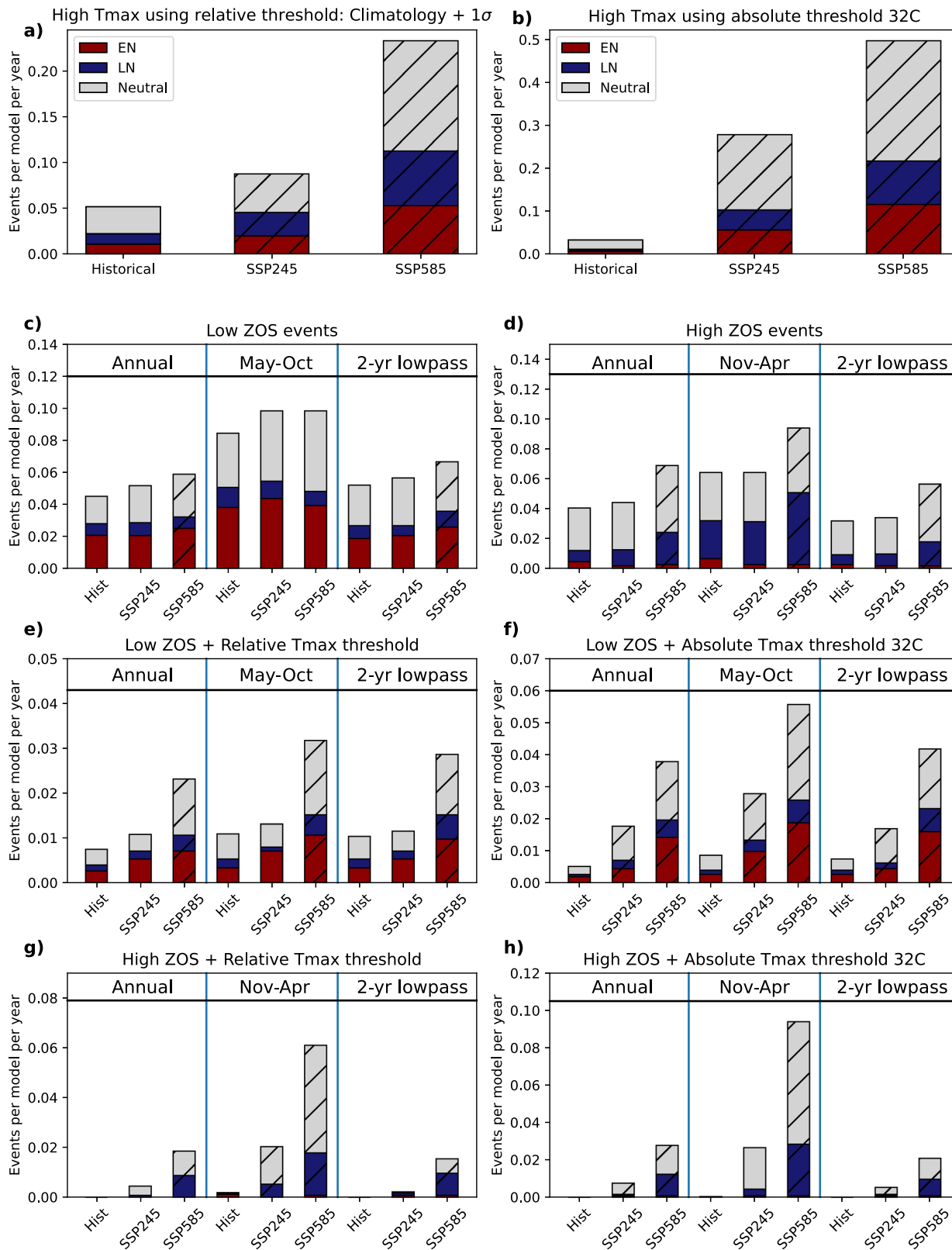
**Fig. 2** Model evaluation of sea level, maximum temperatures and relationship with ENSO in the Gulf of Carpentaria. **a** Gulf of Carpentaria climatological dynamic sea level height above geoid (zos, in metres) for historical (1900–2014; blue), SSP245 (2015–2100; black), and SSP585 (2015–2100; red) scenarios for CMIP6 models. Solid blue, black, and red lines indicate the multi-model mean and shading indicates 1 standard deviation of the model-to-model spread. Solid green line indicates observed climatological monthly mean sea level height. Zos is used as a proxy for modelled sea level variability and absolute values are not comparable to observed sea level height. **b** As for (a), but for monthly means of maximum daily air temperature ( $T_{\max}$ , in degrees Celsius). **c** DJF means of zos in the Gulf of Carpentaria (x-axis) versus the Niño3.4 index (y-axis). The histogram at the top shows the distribution of zos, while the histogram on the right shows the distribution of the Niño3.4 index. Yellow solid line indicates the observed line of best fit (1994–2019). The different scenarios are indicated in blue (historical), black (SSP245), and red (SSP585). **d** As for (c) but for monthly means of maximum daily temperature ( $T_{\max}$ , in degrees). Yellow solid line indicates the observed line of best fit (1950–2019).

to the inability of the models to capture the observed link between ENSO and  $T_{\max}$ , there is no modelled tendency for these high  $T_{\max}$  years to occur more frequently during either El Niño or La Niña, with similar occurrence rates in both (colour in Fig. 3a, b).

The modelled occurrence rates of low sea level events show that there is a heightened risk to mangrove health through anomalous drops in sea level, though the projected increase in risk depends on the period, and the scenario (Fig. 3c). Occurrence rates are calculated for three analysis periods: annual means, May–October dry season means, and annual means of 2-year lowpass-filtered values (zos\_lowfreq; see Methods for definitions). For annual means of zos and zos\_lowfreq, occurrence rates are highest in

SSP585, and changes are statistically significant at the 5% level. For the dry-season May–October means, the increase in occurrence rates are higher but not statistically significant. There are approximately 2–4 times as many low sea level events during El Niño years as compared to La Niña years (Fig. 3c). During El Niño years, rainfall also tends to be anomalously low in the GoC region from approximately September–May<sup>30,31</sup>, which could exacerbate dry conditions towards the beginning or end of the May–October dry season.

Significant changes are also found in the occurrences of anomalous high sea level events (see Methods for definition). For SSP245, the increases are not statistically significant (Fig. 3d).



However, for SSP585, there are significant increases in high sea level events across all three analysis periods, indicating that under this scenario, there is a likely increase in the risk of drowning dieback due to increased seasonal and interannual sea level variability. Again, the models capture more high zos events occurring during La Niña years as compared to El Niño years. During La Niña years, there tends to be an increase in rainfall

from September–May<sup>30,31</sup>, compounding the wet conditions from Nov–April.

Finally, compound heat and sea level stress events are assessed, in which low sea level/high  $T_{max}$  (Fig. 3e–f), or high sea level/high  $T_{max}$  occur during the same year (Fig. 3g, h). Using both relative and absolute thresholds to define  $T_{max}$  years, significant increases are found for all analysis periods under the SSP585 scenario.

**Fig. 3 Projected rates of occurrence of anomalous sea level and high maximum temperature events.** **a** Average number of high  $T_{\max}$  years (normalised, per model, per year) using a relative  $T_{\max}$  threshold (defined in *Methods*; at least 1 month with  $T_{\max} > \text{climatology} + 1\sigma$ ). The colours of the bars correspond to El Niño (red), La Niña (blue), and neutral (grey) years. **b** As for **(a)** but using an absolute threshold of 32 °C to define a high  $T_{\max}$  year. **c** Low sea level events (zos, normalised per model, per year), for annual means, May–October means, and annual means of 2-year lowpass-filtered values. **d** High sea level events (zos, normalised per model, per year), for annual means, November–April means, and annual means of 2-year lowpass-filtered values. **e** Rates of occurrence of years in which low sea level and high  $T_{\max}$  (using the relative threshold) occur concurrently (normalised per model, per year), for annual means, May–October means, and annual means of 2-year lowpass-filtered values. **f** As per **(e)** but using the 32 °C absolute threshold for high  $T_{\max}$  events. **g** Rates of occurrence of years in which high sea level and high  $T_{\max}$  (using the relative threshold, defined in *Methods*) occur concurrently (normalised per model, per year), for annual means and November–April means. **h** As per **(g)** but using the 32 °C absolute threshold for high  $T_{\max}$  events. Hatching in **(a–h)** indicates where the future changes are significant at the 5% level.

During May–October under SSP585, using the absolute  $T_{\max}$  threshold, low sea level/high  $T_{\max}$  events are projected to occur over five times more frequently (Fig. 3f), but using the relative  $T_{\max}$  threshold, compound events are projected to occur approximately 2.5 times more frequently (Fig. 3e). For SSP245, the projected increase in low sea level/high  $T_{\max}$  events is smaller and is only statistically significant in all analysis periods when using the absolute  $T_{\max}$  threshold.

In contrast to the low sea level/high  $T_{\max}$  combination, there are generally fewer high sea level/high  $T_{\max}$  events (Fig. 3h). There are no such events occurring in the historical period for annual means of zos or zos\_lowfreq, and relatively few occurring during November–April. Increases under the SSP245 scenario are small and only significant for November–April using the relative  $T_{\max}$  threshold. However, under the SSP585 scenario the occurrence rates of these events rise markedly, matching those of low sea level/high  $T_{\max}$  events.

The modelled relationship between these compound events and ENSO is somewhat weaker due to the lack of correlation between ENSO and  $T_{\max}$ . However, particularly for SSP585, there is a clear tendency for low sea level/high  $T_{\max}$  events to occur more frequently during El Niño years, and for high sea level/high  $T_{\max}$  events to occur more frequently during La Niña years.

The above findings carry important implications for mangrove communities in a warmer world. Under future projections, both average maximum temperatures and anomalously high  $T_{\max}$  years increase substantially. The smaller occurrence rates of high  $T_{\max}$  years using relative  $T_{\max}$  thresholds imply that if mangrove communities can adapt to a warmer mean state, they would be exposed to relatively fewer high-temperature stress events. However, if they do not adapt and remain physiologically stressed above an absolute  $T_{\max}$  threshold, there is a larger, significant risk of impacts due to high  $T_{\max}$  and compound events under both future scenarios. The projected increase in high temperature events, combined with the projected increase in anomalous low and high sea level events indicate a growing risk of climate factors that severely stress GoC mangroves. This adds to already established global mangrove decline from human-induced land use changes<sup>32</sup> as well as naturally occurring cycles influencing sea level variability<sup>6</sup>. Global efforts towards following a plausible mid-range scenario such as SSP245<sup>33</sup> rather than SSP585, might reduce impacts. However, regardless of scenario, results indicate GoC mangroves will face an increasing threat from climate change. Management and mitigation strategies that reduce stressors are critical in order to minimise impacts to the coastlines, biodiversity and ecosystems that depend on mangrove communities.

## Methods

**Observational data.** For this study, observed sea level data was sourced from the Australian Baseline Sea Level Monitoring Project (<http://www.bom.gov.au/oceanography/projects/abslmp/data/index.shtml>) and observed monthly means of daily maximum temperatures ( $T_{\max}$ ) and rainfall totals were sourced from the Australian Gridded Climate Dataset<sup>34</sup> (AGCD). The observed sea level in the Grootte Eylandt station (Australian Bureau of Meteorology station number 014406)

was used as a proxy for the Gulf of Carpentaria region<sup>4</sup>. The region used for the GoC in this study is 16–14°S, 137–140°E.

**Model output.** Climate model output was sourced from the CMIP6 ensemble of coupled ocean-atmosphere global climate models. The variables examined were relative monthly-mean sea level (zos) and  $T_{\max}$  in the Gulf of Carpentaria (GoC) from simulations of the historical period (1900–2014), and two Shared Socio-economic Pathway (SSP) future scenarios (2015–2100). These scenarios form part of the Coupled Model Intercomparison Phase 6 (CMIP6) database<sup>26</sup>, linked to the recent release of the Intergovernmental Panel on Climate Change sixth assessment. SSP126 is the low-radiative forcing ('best case'; 2.6 W/m<sup>2</sup> by 2100) scenario, from the 'sustainability' narrative in which warming stabilises at ~1.5 degrees. Meanwhile, SSP585 is the high-radiative forcing ('worst case'; 8.5 W/m<sup>2</sup> by 2100) scenario, from the 'fossil fuelled development' narrative, with projected >3 degree warming by 2100<sup>26</sup>. We used the same 13 models for the historical, SSP1-26 and SSP5-85 scenarios (see Appendix). The models were selected based on data availability at the time of analysis.

In the modelled output, the zos variable is defined as being the time-varying sea level anomaly with respect to the geoid. There are two groups of models; one in which the global mean of the zos is always zero, and the other in which the global mean of zos is time-dependent. For consistency between these two groups, we subtracted the global mean zos from each model prior to analysis. This variable therefore represents regional variations in sea level associated with wind, pressure, and circulation patterns such as those associated with ENSO. As the zos values are relative to the global mean sea level, they do not include the global increase in sea level associated with anthropogenic global warming. This may be reasonable as we can assume that GoC mangroves may expand or shift their location in response to this gradual linear increasing sea level trend as evidenced over the decades prior to 2015, whereas stress occurs due to shorter (seasonal-annual) duration events of low sea level such as during 2015–2016<sup>3</sup>. Although evaporative demand is an important indicator of mangrove stress<sup>4</sup>, it is less reliably modelled than sea level and  $T_{\max}$ , so we have not examined it further here.

**Definition of ENSO years.** We defined El Niño and La Niña years using the DJF Niño 3.4 index, which is defined to be the SST anomaly in the region 190–240°E, 5°S–5°N (both with seasonal cycles removed, and SST detrended). A Niño 3.4 index larger than 1 standard deviation indicates an El Niño year, and an index less than negative/minus 1 standard deviation indicates a La Niña year.

To break down stress events into El Niño, La Niña, and neutral phases (Fig. 3), we used the DJF Niño 3.4 index corresponding to the particular year of the event. Noting that DJF spans two calendar years, we used the year corresponding to the beginning of the season (i.e., December).

**Definition of low and high sea level and high temperature events and statistical significance.** As mangroves are stressed by short-lived heat events<sup>8</sup>, and extended periods of low sea level, we used different methods to calculate occurrence rates of low or high sea level and high  $T_{\max}$  events. In this study, we assessed the change in low sea level events over three different time periods: (i) annual means of zos, (ii) May–October means of zos, and (iii) annual means of 2-year lowpass filtered zos. This was to provide an indication of how much the occurrence rates change per year if we considered (i) all months, or (ii) just the dry season (May–October) when sea level is typically lowest. Additionally, we included (iii) because a previous study<sup>4</sup> identified the extended 2-year period of anomalously low sea levels in the GoC as a factor in the dieback event. To do this, we applied a Lanczos filter to the monthly mean data. For high sea level events, we considered November–April means instead, to coincide with the wet season when sea level is typically highest.

As each model has its own range of internal variability, we defined a low sea level event for a particular model as being when the sea level for a particular time mean is lower than  $\text{zos}_{\text{clim}} - 1\sigma$ , where  $\text{zos}_{\text{clim}}$  is that model's climatological value, and  $\sigma$  is the model's standard deviation over the given time mean. To calculate significance of changes to event occurrence rates between scenarios, we used a single sample t-test on the change in the mean number of events for each model.

In the case of  $T_{\max}$ , it only takes a given single month of high  $T_{\max}$  to stress the mangroves. We therefore did not average  $T_{\max}$  over any given period, but counted a high  $T_{\max}$  year as when at least one month per calendar year exceeds a temperature threshold. To account for the modelled Historical  $T_{\max}$  being ~10% cooler than observed, there were two methods we considered in this study. Firstly, we defined a high temperature event when  $T_{\max}$  exceeds an absolute threshold of 32 °C, which is 10% cooler than the observed mangrove threshold of 35 °C. One drawback of this model is that it omits several of the cooler models which do not reach  $T_{\max}$  of 32 °C. The second method was to define a high temperature event for when  $T_{\max}$  exceeds 1 standard deviation of each model's climatological monthly value.

To calculate compound event occurrences, e.g. when low sea level and high temperature occur together, we counted instances of (i) annual means of zos, (ii) May–October means of zos, and (iii) annual means of 2-year lowpass filtered zos, and the number of high  $T_{\max}$  years co-occurring during those periods.

## Data availability

The CMIP6 model output that was analysed in this study are publicly available from <https://esgf-node.llnl.gov/projects/cmip6/>. Observed sea level data is publicly available from the Australian Baseline Sea Level Monitoring Project (<http://www.bom.gov.au/oceanography/projects/abslmp/data/index.shtml>). Observed monthly means of daily maximum temperature and rainfall totals from the Australian Gridded Climate Dataset are publicly available at <https://doi.org/10.4227/1666/5a8647d1c23e0>. All processed data used for the figures are available in Supplementary Data.

## Code availability

Code is available upon request from C.C.

Received: 25 October 2022; Accepted: 16 May 2023;

Published online: 30 May 2023

## References

- Barbier, E. B. et al. The value of estuarine and coastal ecosystem services. *Ecol. Monogr.* **81**, 169–193 (2011).
- Duke, N. C., Hutley, L. B., Mackenzie, J. R. & Burrows, D. in *Processes and Factors Driving Change in Mangrove Forests: An Evaluation Based on the Mass Dieback Event in Australia's Gulf of Carpentaria BT—Ecosystem Collapse and Climate Change* (eds. Canadell, J. G. & Jackson, R. B.) 221–264 (Springer International Publishing, 2021).
- Duke, N. C. et al. ENSO-driven extreme oscillations in mean sea level destabilise critical shoreline mangroves—an emerging threat. *PLOS Clim.* **1**, e0000037 (2022).
- Abhik, S. et al. Influence of the 2015–2016 El Niño on the record-breaking mangrove dieback along northern Australia coast. *Sci. Rep.* **11**, 20411 (2021).
- Sippo, J. Z. et al. Reconstructing extreme climatic and geochemical conditions during the largest natural mangrove dieback on record. *Biogeosciences* **17**, 4707–4726 (2020).
- Saintilan, N. et al. The lunar nodal cycle controls mangrove canopy cover on the Australian continent. *Sci. Adv.* **8**, eabo6602 (2022).
- Harris, R. M. B. et al. Biological responses to the press and pulse of climate trends and extreme events. *Nat. Clim. Chang.* **8**, 579–587 (2018).
- Lovelock, C. E., Krauss, K. W., Osland, M. J., Reef, R. & Ball, M. C. *The Physiology of Mangrove Trees with Changing Climate BT—Tropical Tree Physiology: Adaptations and Responses in a Changing Environment* (eds. Goldstein, G. & Santiago, L. S.) 149–179 (Springer International Publishing, 2016).
- Feller, I. C. et al. Biocomplexity in mangrove ecosystems. *Ann. Rev. Mar. Sci.* **2**, 395–417 (2010).
- Krauss, K. W. et al. How mangrove forests adjust to rising sea level. *New Phytol.* **202**, 19–34 (2014).
- Holbrook, N. J. et al. ENSO-Driven Ocean Extremes and Their Ecosystem Impacts. *El Niño Southern Oscillation in a Changing Climate* 409–428 <https://doi.org/10.1002/9781119548164.ch18> (2020).
- Bindoff, N. L. et al. in *IPCC Special Report on the Ocean and Cryosphere in a Changing Climate* (eds. Portner, H.-O. et al.) 447–587 (Cambridge University Press, 2019) <https://doi.org/10.1017/9781009157964.007>.
- Zinke, J., Rountrey, A. & Feng, M. et al. Corals record long-term Leeuwin current variability including Ningaloo Niño/Niña since 1795. *Nat. Commun.* **5**, 3607 (2014).
- Allen, K. J., Verdon-Kidd, D. C., Sippo, J. Z. & Baker, P. J. Compound climate extremes driving recent sub-continental tree mortality in northern Australia have no precedent in recent centuries. *Sci. Rep.* **11**, 18337 (2021).
- Lovelock, C. E., Feller, I. C., Reef, R., Hickey, S. & Ball, M. C. Mangrove dieback during fluctuating sea levels. *Sci. Rep.* **7**, 1680 (2017).
- Rodríguez, J. F., Saco, P. M., Sandi, S., Saintilan, N. & Riccardi, G. Potential increase in coastal wetland vulnerability to sea-level rise suggested by considering hydrodynamic attenuation effects. *Nat. Commun.* **8**, 1–12 (2017).
- Waddington, K., Khojasteh, D., Marshall, L., Rayner, D. & Glamore, W. Quantifying the effects of sea level rise on estuarine drainage systems. *Water Resources Res.* **58**, e2021WR031405 (2022).
- Brocklehurst, P. S. & Edmeades, B. F. Mangrove Survey of Darwin Harbour, Northern Territory, Australia, Technical Report No. R96/7 Department of Lands, Planning and Environment, NT (1996)
- Lee, G.P. Mangroves in the Northern Territory, Department of Infrastructure, Planning and Environment, Darwin (2003),
- Zheng, Y. & Takeuchi, W. Estimating mangrove forest gross primary production by quantifying environmental stressors in the coastal area. *Sci. Rep.* **12**, 2238 (2022).
- Ball, M. C. Ecophysiology of mangroves. *Trees* **2**, 129–142 (1988).
- Martínez-Díaz, M. G. & Reef, R. A biogeographical approach to characterizing the climatic, physical and geomorphic niche of the most widely distributed mangrove species, *Avicennia marina*. *Diversity Distributions* **29**, 89–108 (2022).
- Andrews, T. J. & Muller, G. J. Photosynthetic gas exchange of the Mangrove, *Rhizophora stylosa* Griff., in Its Natural Environment. *Oecologia* **65**, 449–455 (1985).
- Cheeseman, J. M. et al. The analysis of photosynthetic performance in leaves under field conditions: a case study using *Bruguiera* mangroves. *Photosynth. Res.* **29**, 11–22 (1991).
- Flato, G. et al. in *Evaluation of climate models BT—Climate Change 2013: The Physical Science Basis. Contribution of Working Group I to the Fifth Assessment Report of the Intergovernmental Panel on Climate Change* (eds. Stocker, T. F. et al.) 741–882 (Cambridge University Press, 2013).
- Eyring, V., Bony, S., Meehl, G. A., Senior, C. A., Stevens, B., Stouffer, R. J. & Taylor, K. E. Overview of the Coupled Model Intercomparison Project Phase 6 (CMIP6) experimental design and organization. *Geosci. Model Dev.* **9**, 1937–1958 (2016).
- Oliver, E. C. J. & Thompson, K. R. Sea level and circulation variability of the Gulf of Carpentaria: Influence of the Madden-Julian Oscillation and the adjacent deep ocean. *J. Geophys. Res. Ocean.* **116**, (2011).
- Harris T, Hope P, Oliver E, Smalley R, Arblaster J, Holbrook N, Duke N, Pearce K, Braganza, K and Bindoff N. Climate drivers of the 2015 Gulf of Carpentaria mangrove dieback. Earth Systems and Climate Change Hub Technical Report No. 2, NESP Earth Systems and Climate Change Hub, Australia 2017.
- Cai, W. et al. Increased ENSO sea surface temperature variability under four IPCC emission scenarios. *Nat. Clim. Chang.* **12**, 228–231 (2022).
- Risbey, J. S., Pook, M. J., McIntosh, P. C., Wheeler, M. C. & Hendon, H. H. On the Remote Drivers of Rainfall Variability in Australia. *Monthly Weather Review* **137**, 3233–3253 (2009).
- Chung, C. & Power, S. The non-linear impact of El Niño, La Niña and the Southern Oscillation on seasonal and regional Australian precipitation. *J. South. Hemisphere Earth Syst. Sci.* **67**, 25–45 (2017).
- Goldberg, L., Lagomasino, D., Thomas, N. & Fatoyinbo, T. Global declines in human-driven mangrove loss. *Glob. Chang. Biol.* **26**, 5844–5855 (2020).
- Pielke, R. Jr & Burgess, M. G. & Ritchie, J. Plausible 2005–2050 emissions scenarios project between 2 °C and 3 °C of warming by 2100. *Environ. Res. Lett.* **17**, 24027 (2022).
- Evans, A., Jones, D., Smalley, R. & Lelyst, S. *An Enhanced Gridded Rainfall Analysis Scheme for Australia* (2020).

## Acknowledgements

The authors wish to thank anonymous reviewers, Claire Spillman, Sugata Narsey, and David Jones for helpful reviews of the manuscript. The authors are also grateful to Francois Delage for processing, and regridding the CMIP6 data, and for providing scripts to read in the data. We also thank Francois Delage, Sugata Narsey, and Ghyslaine Boschat for useful discussions on statistical and data visualisation methods. The authors also thank Wasył Drosdowsky for his work exploring the timing of the tides in the Gulf, Abhik Santra, Marycarmen Martinez-Diaz and Ruth Reef for useful discussions. We thank the Northern Territory Government of Australia for their partial funding of this project. This project was supported with funding from the Australian Government's National Environmental Science Program and undertaken with the assistance of resources and services from the National Computational Infrastructure (NCI), which is supported by the Australian Government.

## Author contributions

All authors (C.C., P.H., L.H., N.D., J.B.) contributed to the design and interpretation of the analysis, and reviewing of the manuscript. C.C. ran the analysis, and contributed to writing the manuscript and production of the figures. P.H. conceived the project and

contributed to writing the manuscript. L.H. contributed to writing the manuscript. N.D. took the image in Fig. 1b.

### Competing interests

The authors declare no competing interests.

### Additional information

**Supplementary information** The online version contains supplementary material available at <https://doi.org/10.1038/s43247-023-00852-z>.

**Correspondence** and requests for materials should be addressed to Christine T. Y. Chung.

**Peer review information** *Communications Earth & Environment* thanks Kerry Lee Rogers and the other, anonymous, reviewer(s) for their contribution to the peer review of this work. Primary Handling Editors: Christopher Cornwall and Aliénor Lavergne.

**Reprints and permission information** is available at <http://www.nature.com/reprints>

**Publisher's note** Springer Nature remains neutral with regard to jurisdictional claims in published maps and institutional affiliations.



**Open Access** This article is licensed under a Creative Commons Attribution 4.0 International License, which permits use, sharing, adaptation, distribution and reproduction in any medium or format, as long as you give appropriate credit to the original author(s) and the source, provide a link to the Creative Commons license, and indicate if changes were made. The images or other third party material in this article are included in the article's Creative Commons license, unless indicated otherwise in a credit line to the material. If material is not included in the article's Creative Commons license and your intended use is not permitted by statutory regulation or exceeds the permitted use, you will need to obtain permission directly from the copyright holder. To view a copy of this license, visit <http://creativecommons.org/licenses/by/4.0/>.

© Crown 2023